Journal of Power Sources 265 (2014) 149–159

Contents lists available at ScienceDirect

Journal of Power Sources

journal homepage: www.elsevier.com/locate/jpowsour

Improving long-term operation of power sources in off-grid hybrid systems based on renewable energy, hydrogen and battery

Pablo García [a], Juan P. Torreglosa [b,c], Luis M. Fernández [a,*], Francisco Jurado [b]

[a] Research Group in Electrical Technologies for Sustainable and Renewable Energy (PAIDI-TEP-023), Department of Electrical Engineering, EPS Algeciras, University of Cadiz, Avda. Ramón Puyol, s/n., 11202 Algeciras, Cádiz, Spain
[b] Research Group in Research and Electrical Technology (PAIDI-TEP-152), Department of Electrical Engineering, EPS Linares, University of Jaen, C/ Alfonso X, n° 28., 23700 Linares, Jaén, Spain
[c] Universidad Autónoma de Chile, Avenida Alemania 01090, Temuco, Chile

HIGHLIGHTS

- We present two energy supervisory controls for improving long-term operation of off-grid hybrid systems.
- Battery SOC, hydrogen tank level and remaining energy of storage devices were considered by the controls.
- The controls were tested by simulation along the expected lifetime of the hybrid system.
- The results demonstrated the feasibility of the controls for off-grid applications.

ARTICLE INFO

Article history:
Received 25 December 2013
Received in revised form
4 April 2014
Accepted 24 April 2014
Available online 2 May 2014

Keywords:
Renewable energy
Hybrid system
Hydrogen
Supervisory control

ABSTRACT

This paper presents two novel hourly energy supervisory controls (ESC) for improving long-term operation of off-grid hybrid systems (HS) integrating renewable energy sources (wind turbine and photovoltaic solar panels), hydrogen system (fuel cell, hydrogen tank and electrolyzer) and battery. The first ESC tries to improve the power supplied by the HS and the power stored in the battery and/or in the hydrogen tank, whereas the second one tries to minimize the number of needed elements (batteries, fuel cells and electrolyzers) throughout the expected life of the HS (25 years). Moreover, in both ESC, the battery state-of-charge (SOC) and the hydrogen tank level are controlled and maintained between optimum operating margins. Finally, a comparative study between the controls is carried out by models of the commercially available components used in the HS under study in this work. These ESC are also compared with a third ESC, already published by the authors, and based on reducing the utilization costs of the energy storage devices. The comparative study proves the right performance of the ESC and their differences.

© 2014 Elsevier B.V. All rights reserved.

1. Introduction

Nowadays problems related with the lack of electrical grid in inaccessible areas due to the operating cost can be solved installing off-grid system. Usually, since years ago, most of off-grid systems have been based on diesel engines as primary energy sources [1,2]. However, due to the low maintenance and operation cost and the long expected life, off-grid system based on renewable energy is becoming an alternative to the classical off-grid system. Normally, in these new systems, the renewable energy is composed of photovoltaic solar panels (PV), wind turbines (WT) or both, so that they do not emit greenhouse gases, they are low pollution energy sources [3] and they avoid the use of fossil fuel [4].

However, the energy production from the sun and from the wind do not always coincide with the power demand, and therefore, energy secondary systems must be used together with the renewable energy sources for energy support/storage [5,6]. These secondary systems are typically batteries and hydrogen systems, composed by fuel cell (FC) electrolyzer and hydrogen tank, but also super-capacitors or superconducting magnetic energy storage (SMES) [7] can be used [8]. For example, the storage and support system was integrated by hydrogen system (FC, electrolyzer and hydrogen tank) in Ref. [9]; by battery pack in Ref. [10]; and by hydrogen system and battery in Ref. [11]. Otherwise, some studies

* Corresponding author. Tel.: +34 956 02 81 66; fax: +34 956 02 80 01.
E-mail addresses: pablo.garcia@uca.es (P. García), jtorregl@ujaen.es (J. P. Torreglosa), luis.fernandez@uca.es (L.M. Fernández), fjurado@ujaen.es (F. Jurado).

http://dx.doi.org/10.1016/j.jpowsour.2014.04.118
0378-7753/© 2014 Elsevier B.V. All rights reserved.

Nomenclature

CAP_{H2}	tank nominal capacity, (kg)
DOD_{nom}	nominal depth of discharge for the battery, (%)
$E_{bat,char}$	battery charge energy, (Wh)
$E_{bat,dis}$	battery discharge energy, (Wh)
E_{bat}^{nom}	battery nominal capacity, (Wh)
E_{fc}	FC energy, (Wh)
$E_{low,H2}$	hydrogen lower heating value, (Wh kg^{-1})
E_{lz}	electrolyzer energy, (Wh)
ESC	energy supervisory control
ESC,1	superscript for the equations related to the first ESC
ESC,2	superscript for the equations related to the second ESC
E_{un}	unused energy, (Wh)
$H2_{avg}$	average hydrogen level of the tank, (%)
$H2_{min}$	minimum hydrogen level of the tank, (%)
H_{fc}	electrolyzer current number of working hours, (h)
H_{fc}	FC current number of working hours, (h)
H_{fc}	working hours of the FC, (h)
H_{fc}^{life}	FC expected life, (h)
H_{fc}^{life}	FC lifetime, (h)
H_{lz}^{life}	electrolyzer expected life, (h)
H_{lz}^{life}	electrolyzer lifetime, (h)
H_{lz}	working hours of the electrolyzer, (h)
HS	hybrid system
H_{warr}	FC working hours defined by the warranty, (h)
$K_{bat,char}$	battery system charge constant, (−)
$K_{bat,des}$	battery system discharge constant, (−)
$K_{H2,char}$	hydrogen system charge constant, (−)
$K_{H2,des}$	hydrogen system discharge constant, (−)
L_{H2}	level of the hydrogen tank, (%)
N_{bat}	number of batteries used throughout the lifetime of the HS, (−)
N_{cycles}	number of complete cycles of the battery, (−)
N_{fc}	number of FC used throughout the lifetime of the HS, (−)
N_{cycles}^{life}	maximum charge/discharge cycles that the battery can complete during its life, (−)
N_{lz}	number of electrolyzers used throughout the lifetime of the HS, (−)
P_{bat}^{*}	ideal battery power, (W)
P_{fc}^{*}	ideal fuel cell power, (W)
P_{lz}^{*}	ideal electrolyzer power, (W)
P_1	time that the ECS have been working in the state 1, (%)
P_{48}	time that the ECS have been working in the states 4 and 8, (%)
P_5	time that the ECS have been working in the state 5, (%)
$P_{bat,charg}^{av}$	battery available power during a charge in the next hour, (W)
$P_{bat,dis}^{av}$	battery available power during a discharge in the next hour, (W)
P_{char}^{av}	maximum power that the FC together with the battery can absorb, (W)
P_{dis}^{av}	maximum power that the FC together with the battery can deliver, (W)
$P_{H2,fc}^{av}$	maximum power that the FC can deliver in the next hour, (W)
$P_{H2,lz}^{av}$	maximum power that the electrolyzer can store in the next hour, (W)
P_{bat}	battery output power, (W)
P_{bat}^{max}	battery maximum power, (W)
P_{extra}	extra power, (W)
P_{fc}	FC output power, (W)
P_{fc}^{rtd}	FC rated power, (W)
P_{lz}	electrolyzer output power, (W)
P_{lz}^{rtd}	electrolyzer rated power, (W)
P_{net}	net power, (W)
PV	photovoltaic solar panel
S	state, (−)
SOC	state of charge
SOC_{avg}	average battery SOC, (%)
SOC_{min}	minimum SOC allowed
t	duration of the battery power exchange, (h)
Δt	interval time between two simulation steps, (h)

about the performance of off-grid system were detailed in Refs. [12–14].

Furthermore, due to the imbalance between the demanded power and the power generated by the renewable energy system, an ESC is necessary for the optimal energy flow of the energy sources within the HS, whose main goal must be supply the load. Normally, the common ESC are based on flowchart, because they are easy to implement and really effective. Examples of ESC based on flowcharts applied to HS can be found in Refs. [15–20]. On the other hand, ESC not based on flowcharts have been also used [3,21–23]. An ESC based on PI controllers was used in Ref. [3]. A simple ESC based on the available energy and the energy demanded by the load was applied in Ref. [21]. An ESC based on mixed-integer linear programming was detailed in Ref. [22]. A genetic algorithm was developed in Ref. [23] for sizing and optimizing the energy flow of a daily load. Nevertheless, there are few works in which the performance of the ESC have been studied over long periods. The ESC is evaluated along one year in Refs. [18] and [23], along one week in Ref. [24], and along 24 h in Ref. [25].

This work presents two novel ESC for off-grid HS. The ESC are applied to a HS composed of PV panels, WT, and battery and hydrogen system (FC, electrolyzer and hydrogen), They are tested throughout the expected life of the HS (25 years) and compared with the ESC developed by the authors in Ref. [20] with the objective of reducing the utilization costs of the battery and hydrogen system. The first ESC tries to improve the generated and stored energy of the HS, whereas the second one is focused on minimizing the number of needed elements through the expected life of the HS. Thus, once concluded the introduction, this paper is structured as follows. The configuration of the off-grid HS used for the development of the two ESC is presented in Section 2. Section 3 details the two novel ESC, and develops briefly the ESC presented in Ref. [20]. Section 4 presents the real components of the HS used to test the performance of the ESC. A comparative study among the three ESC is carried out in Section 5, and finally, the paper ends with the conclusions in Section 6.

2. Off-grid HS configuration

The two novel ESC can be applied to several configurations of an off-grid HS. One suitable configuration is showed in Fig. 1, which is used for studying and comparing the ESC presented in this paper. According to this configuration, the renewable energy system, composed of WT and PV panels, acts as primary energy source. In

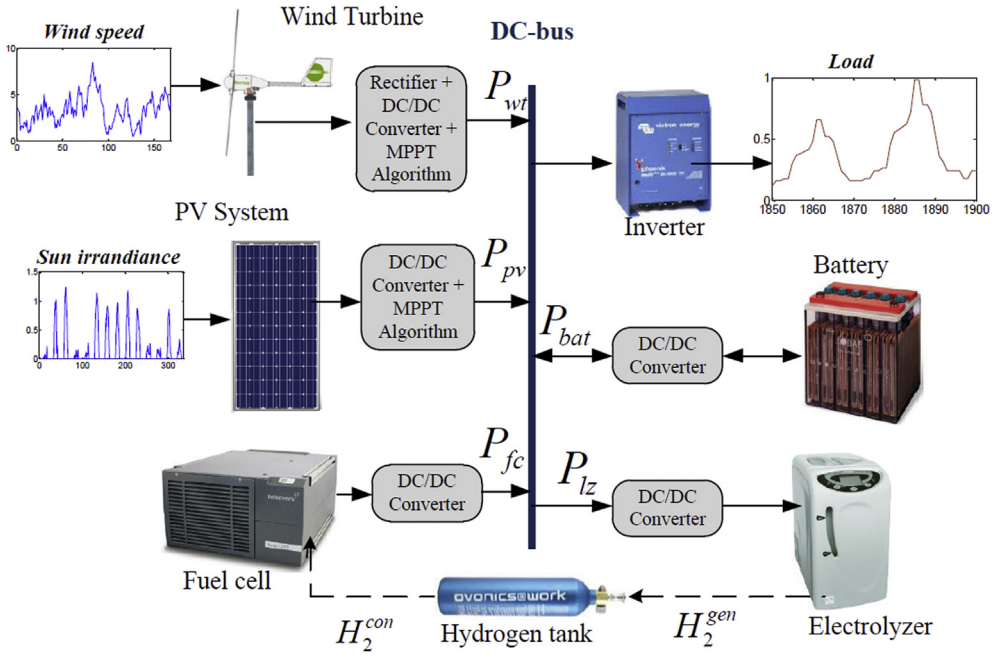

Fig. 1. Off-grid HS configuration.

both cases, the WT and PV panels are connected to the DC bus voltage through DC/DC converters, which use MPPT controllers to extract the maximum available power from the wind and sun irradiance, respectively.

Otherwise, the battery and the hydrogen system are used to support the renewable energy system and to store the power generated by the renewable system and not used by the load. Thus, if the demanded load is higher than the power generated by the WT and PV panels, the battery or the FC must generate this power deficit. On the contrary, if the demanded load is smaller than the renewable power, this extra power is used by the electrolyzer to generate hydrogen or it is stored in the battery. In all the cases, in order to achieve an appropriate energy flow, each energy source is connected to the DC bus through a controllable DC/DC power converter.

3. Energy supervisory controls (ESC)

As it was commented above, the power generated by the renewable energy sources does not correspond sometimes with the demanded load, and therefore the battery or the hydrogen system must work. The difference between the power demanded by the load and the power generated by the renewable energy sources is defined as the net power, which can be positive or negative. The ESC has to decide if the net power is generated or absorbed by the battery or by the hydrogen system or by both, and, moreover, to control the battery SOC and the hydrogen level between optimum operating margins.

Fig. 2 presents a scheme of the overall configuration used for the two new ESC. The main difference between both controls is the way of calculating the remaining energy of the battery (battery charge energy, $E_{bat,char}$, and battery discharge energy, $E_{bat,dis}$) and hydrogen system (FC energy, E_{fc}, and electrolyzer energy, E_{lz}). Section 3.1 shows the common blocks for both ESC, and Sections 3.2 and 3.3 detail the way of obtaining the remaining energies in the two ESC. In general, both ESC try to generate or absorb the net power with the battery and the hydrogen system by applying a proportional division of the net power between them taking into account the values of remaining energy, as shown further on.

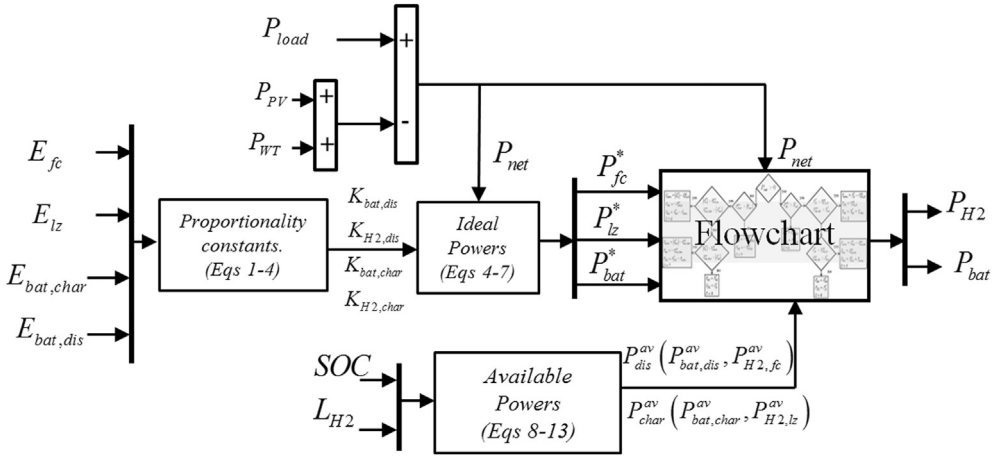

Fig. 2. Scheme of the overall configuration used for the two new ESC.

Finally, Section 3.4 describes briefly the third ESC, already presented in Ref. [20]. This third ESC based on flowchart and fuzzy logic presents a different approach. It was designed to decrease the utilization costs of the battery and hydrogen system. In fact, this ESC and the other two novel ESC, in which the utilization costs have not been taken into account, are compared in this work in order to show the differences among them.

3.1. Development of the ESC: common blocks

According to Fig. 2, the common blocks of the new ESC are the following ones: proportionality constants, ideal power, maximum available power calculation and flowchart. Next, all these blocks are commented.

3.1.1. Proportionality constants

As commented above, the ESC are based on a proportional division of the net power. Thus, in both controls during a discharge, the proportional constants are obtained as follows:

$$K_{bat,dis} = \frac{E_{bat,dis}}{E_{bat,dis} + E_{fc}} \quad (1)$$

$$K_{H2,dis} = \frac{E_{fc}}{E_{bat,dis} + E_{fc}} \quad (2)$$

where $K_{bat,dis}$ and $K_{H2,dis}$ are the battery and the hydrogen system discharge constants.

In the same way, during charging process the proportional constants are the following.

$$K_{bat,char} = \frac{E_{bat,char}}{E_{bat,char} + E_{lz}} \quad (3)$$

$$K_{H2,char} = \frac{E_{lz}}{E_{bat,char} + E_{lz}} \quad (4)$$

where $K_{bat,char}$ and $K_{H2,char}$ are the battery and the hydrogen system discharge constants.

3.1.2. Ideal powers

Once obtained the proportional constants, the ideal battery power and the ideal hydrogen system power (FC and electrolyzer power) are calculated. These powers are proportional to the net power, as expressed in Eqs (5)–(7), and they would be the power to be generated by/stored in the battery and/or hydrogen system if the battery SOC and the hydrogen tank level were not controlled.

$$P^*_{bat} = \begin{cases} K_{bat,dis} \times P_{net} & \text{with } P_{net} > 0 \\ K_{bat,char} \times P_{net} & \text{with } P_{net} \le 0 \end{cases} \quad (5)$$

$$P^*_{fc} = K_{H2,dis} \times P_{net} \quad (6)$$

$$P^*_{lz} = K_{H2,char} \times P_{net} \quad (7)$$

3.1.3. Maximum available powers calculation

The maximum available powers are the maximum powers of the battery, FC and electrolyzer, which are defined to avoid an over charge or over discharge of the battery and the hydrogen tank during the next simulation step (one hour). Furthermore, the maximum available powers in a discharge and in a charge are defined as follows. In the next simulation hour, P^{av}_{dis} is the maximum power that the FC together with the battery can deliver, whereas P^{av}_{char} is the maximum power that the battery and the electrolyzer can absorb.

$$P^{av}_{dis} = P^{av}_{bat,dis} + P^{av}_{H2,fc} \quad (8)$$

$$P^{av}_{char} = P^{av}_{bat,char} + P^{av}_{H2,lz} \quad (9)$$

where $P^{av}_{bat,charg}$, $P^{av}_{bat,dis}$ are battery available power during a charge or discharge in the next hour; $P^{av}_{H2,fc}$ is the maximum power that the FC can deliver in the next hour (available power in the hydrogen tank); and $P^{av}_{H2,lz}$ is the maximum power that the electrolyzer can store in the tank in the next simulation step. $P^{av}_{bat,char}$, $P^{av}_{bat,dis}$ can be obtained according to Eqs. (10) and (11), respectively [26]. $P^{av}_{bat,char}$ is the minimum value between the maximum power and the maximum charge power of the battery, which depends on the SOC. $P^{av}_{bat,dis}$ is the minimum value between the maximum power and the maximum power that the battery could deliver for avoiding a SOC below the minimum value allowed to it (SOC_{min}).

$$P^{av}_{bat,char} = \min\left(P^{max}_{bat}, \frac{E^{nom}_{bat}}{\Delta t} \times \left(\frac{100 - SOC}{100}\right)\right) \quad (10)$$

$$P^{av}_{bat,dis} = \min\left(P^{max}_{bat}, \frac{E^{nom}_{bat}}{\Delta t} \times \left(\frac{SOC - SOC_{min}}{100}\right)\right) \quad (11)$$

where E^{nom}_{bat} represents the battery nominal capacity in energy terms; P^{max}_{bat} is the battery maximum power defined by the manufacturer [27]; and Δt is the interval time between two simulation steps.

Regarding the hydrogen system, the maximum power that the FC and the electrolyzer can deliver or absorb during the next simulation step is related with the current level of the hydrogen tank. Thereby, the FC maximum available power is calculated from the minimum value between the FC rated power (P^{rtd}_{fc}) and the maximum power that the FC could generate according to current level of the hydrogen tank (L_{H2}).

$$P^{av}_{H2,fc} = \min\left(P^{rtd}_{fc}, E_{low,H2} \cdot \eta_{therm} \cdot U_f \cdot \eta_{stack} \cdot \frac{CAP_{H2}}{\Delta t} \times \frac{L_{H2}}{100}\right) \quad (12)$$

where $E_{low,H2}$ is the hydrogen lower heating value; CAP_{H2} is the tank nominal capacity in kilograms; η_{therm}, U_f and η_{stack} are specific parameters of the FC, which depend on the selected FC; η_{therm} is the thermodynamic efficiency; U_f is the FC utilization factor [28]; and η_{stack} is the FC stack efficiency, which is calculated as the ratio between the output stack voltage and the standard-state reversible voltage.

With respect to the electrolyzer, the maximum available power that can be absorbed during a certain hour is calculated from the minimum value between the electrolyzer rated power (P^{rtd}_{lz}) and the power that could produce a complete filling of the hydrogen tank.

$$P^{av}_{H2,lz} = \min\left(P^{rtd}_{lz}, B \cdot q^{nom}_{H2} + A \cdot \frac{CAP_{H2}}{\Delta t} \cdot \left(\frac{100 - L_{H2}}{100}\right)\right) \quad (13)$$

where A and B are coefficients of the selected electrolyzer model [29]; and q^{nom}_{H2} is the electrolyzer rated hydrogen.

3.1.4. Flowchart

Finally, because of the battery SOC and hydrogen tank level must be controlled, a controller based on flowchart, common for both ESC, is developed. The inputs of this flowchart are the ideal power of the battery and hydrogen system (P^*_{bat}, P^*_{fc} and P^*_{lz}), the net

power (P_{net}), and the maximum available powers during a discharge and charge (P^{av}_{dis} and P^{av}_{char}). The outputs are the battery, FC and electrolyzer powers (P_{bat}, P_{fc} and P_{lz}).

Note that, by using the maximum available powers, the battery SOC and the hydrogen level can be controlled and the power generated/absorbed by the battery and by the hydrogen system can be optimized. Fig. 3 shows the flowchart and Table 1 presents a summary of the different control states used in both ESC. During a discharge process ($P_{net} > 0$), the flowchart works in the following way. If P^{av}_{dis} is smaller than P_{net}, then the battery and FC must generate theirs maximum available powers ($P^{av}_{bat,dis}$ and $P^{av}_{H2,fc}$). In this state ($S = 1$), the HS system cannot generate the power demanded by the load, and therefore, this state must be avoided. On the contrary, if P^{av}_{dis} is higher than P_{net}, the power demanded by load can be generated. Now, if the battery maximum available power is higher than the ideal battery power ($P^{av}_{bat,dis} > P^{*}_{bat}$) but the FC maximum power is smaller than the FC ideal power ($P^{av}_{H2,fc} < P^{*}_{fc}$), the FC must deliver its maximum power and the battery must generate the ideal battery power plus an extra power (P_{extra}) in order to provide the net power. This is named as state 2 ($S = 2$). Otherwise, if the previous conditions are not achieved, the opposite case happens ($P^{av}_{bat,dis} < P^{*}_{bat}$ and $P^{av}_{H2,fc} > P^{*}_{fc}$). In this state ($S = 3$), the battery must generate its maximum available power and the FC has to generate the FC ideal power plus the extra power. If this latter condition neither occurs, then the maximum available powers are higher than the ideal powers ($P^{av}_{bat,dis} > P^{*}_{bat}$ and $P^{av}_{H2,fc} > P^{*}_{fc}$). This last case ($S = 4$) must be the more usual state, in which the battery and FC way deliver their ideal powers.

Finally, if P_{net} is smaller than 0, the flowchart works in a similar way as explained above. Thus, the battery and the electrolyzer absorb the ideal powers only if the following two conditions are achieved: $P^{av}_{bat,char} < |P^{*}_{bat}|$ and $P^{av}_{H2,lz} < |P^{*}_{lz}|$, ($S = 8$).

Table 1
Summary of the control states used in the flowchart of the ESC 1 and ESC 2.

S	P_{bat}	P_{H2}
$\boldsymbol{P_{net} > 0}$		
1	$P^{av}_{bat,dis}$	$P^{av}_{H2,dis}$
2	$P^{*}_{bat} + P_{extra} = P^{*}_{bat} + (P^{*}_{fc} - P^{av}{}_{H2,fc})$	$P^{av}_{H2,fc}$
3	$P^{av}_{bat,dis}$	$P^{*}_{H2} + P_{extra} = P^{*}_{H2} + (P^{*}_{bat} - P^{av}{}_{bat,dis})$
4	P^{*}_{bat}	P^{*}_{fc}
$\boldsymbol{P_{net} < 0}$		
5	$-P^{av}_{bat,char}$	$-P^{av}_{H2,fc}$
6	$P^{*}_{bat} - P_{extra} = P^{*}_{bat} - (|P^{*}_{lz}| - P^{av}{}_{H2,lz})$	$-P^{av}_{H2,lz}$
7	$-P^{av}_{bat,char}$	$P^{*}_{H2} - P_{extra} = P^{*}_{H2} - (|P^{*}_{bat}| - P^{av}{}_{bat,char})$
8	P^{*}_{bat}	P^{*}_{fc}

3.2. ESC 1

This control tries to improve the power flow of the HS avoiding the state 1 of the flowchart and to store most of the renewable energy in the hydrogen tank and/or in the battery. It calculates the remaining energy of the battery ($E_{bat,char}$ and $E_{bat,dis}$) and hydrogen system (E_{fz} and E_{lz}) from the battery SOC and the hydrogen tank. In this case, during a discharge, the battery available energy is calculated taking into account the corresponding energy to the difference between the current SOC and the minimum SOC allowed to the battery (SOC_{min}). In the same way, during a charge, the energy considered by the control is the maximum energy that the battery can store from the current SOC to a complete charge of the battery. For this control, all the energy terms are denoted as ESC,1 in the superscripts.

$$E^{ECS,1}_{bat,dis} = \frac{DOD_{nom}}{100} \times E_{bat,nom} \times (SOC - SOC_{min}) \quad (14)$$

$$E^{ECS,1}_{bat,char} = \frac{DOD_{nom}}{100} \times E_{bat,nom} \times (100 - SOC) \quad (15)$$

where $E_{bat,nom}$ is the battery nominal capacity in energy terms; and DOD_{nom} represents the nominal Depth of Discharge (DOD) recommended for the battery.

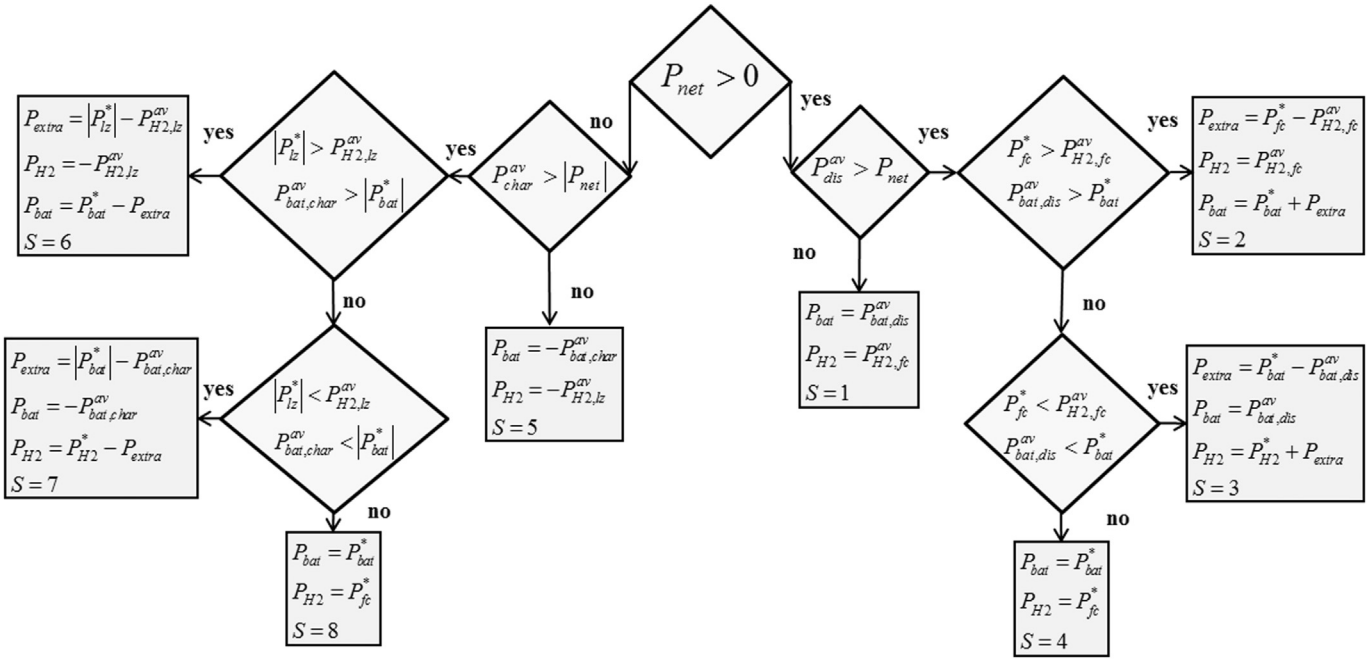

Fig. 3. Flowchart control.

Regarding the hydrogen system, the remaining energies are calculated by Eqs. (16) and (17). Eq. (16) represents the total energy that the FC could generate according to the current hydrogen level. Eq. (17) defines the maximum energy that the electrolyzer could store in the hydrogen tank according from the current hydrogen level.

$$E_{fc}^{ECS,1} = E_{low,H2} \cdot \eta_{therm} \cdot U_f \cdot \eta_{stack}^{avg} \cdot CAP_{H2} \times \frac{L_{H2}}{100} \quad (16)$$

$$E_{lz}^{ECS,1} = B \cdot CAP_{H2} + A \cdot CAP_{H2} \cdot \left(\frac{100 - L_{H2}}{100}\right) \quad (17)$$

where η_{stack}^{avg} is the average stack efficiency.

Note that, with this ESC, the battery SOC and the hydrogen level will evolve in a similar way, so that the load supply could be guaranteed whenever there was energy available stored in the battery and the hydrogen tank. For example, during a positive net power (power to be generated), the energy source with more energy stored will have to deliver more power than the other energy source in order to control the battery SOC and the hydrogen tank level.

3.3. ESC 2

This control tries to minimize the number of needed elements (batteries, FC and electrolyzers) throughout the expected life of the HS. In this case, the remaining energy of the battery and hydrogen system depend on the total quantity of energy that the battery or the hydrogen system can absorb or deliver along their whole life, which decreases as the elements become older. Thereby, the control needs to know parameters such as the current number of complete cycles of the battery (N_{cycles}) and the working hours of the FC and electrolyzer (H_{fc}, H_{lz}). Because of the battery SOC and the hydrogen level are not needed to calculate the remaining energy terms, the flowchart is essential to control these levels.

The battery energy terms, denoted for this control with ESC,2 in the superscripts, are obtained from Eqs. (18) and (19). In this case, the considered energy corresponds to the total remaining energy throughout the lifetime of the battery. Thus, as the battery is completing cycles, the remaining energy is decreasing and it will be used less than at the beginning of its life, as the battery gets older. Moreover, the remaining energy is considered the same in the charging and discharging process.

$$E_{bat,dis}^{ECS,2} = 0.5 \times E_{bat,nom} \times \frac{DOD_{nom}}{100}\left(N_{cycles}^{life} - N_{cycles}\right) \quad (18)$$

$$E_{bat,char}^{ECS,2} = E_{bat,dis}^{ECS,2} \quad (19)$$

where N_{cycles}^{life} are the maximum cycles of charge and discharge that the battery can complete during its life.

The FC energy is obtained from the product of the total energy that the FC can generate from the hydrogen stored in the tank – the first term in brackets in Eq. (20) – and the difference between the FC expected life in working hours (H_{fc}^{life}) and the current number of working hours (H_{fc}), which is divided by the time in hours that the FC takes in consuming the entire hydrogen tank when the FC is generating its rated power.

Similarly, the electrolyzer energy is calculated from the product of the maximum quantity of energy that can be stored in the hydrogen tank – the first term in brackets in Eq. (21) – and the difference between the electrolyzer expected life in working hours (H_{lz}^{life}) and the current number of working hours (H_{lz}), which is divided by the time in hours (rt_{lz}^{life}) that the electrolyzer takes in completing a charge cycle of the hydrogen tank.

$$E_{fc}^{ECS,2} = \left[E_{low,H2} \cdot \eta_{therm} \cdot U_f \cdot \eta_{stack}^{avg} \cdot CAP_{H2}\right]\left(\frac{H_{fc}^{life} - H_{fc}}{rt_{fc}^{life}}\right) \quad (20)$$

$$E_{lz}^{ECS,2} = \left[B \cdot q_{H2}^{nom} + A \cdot CAP_{H2}\right]\left(\frac{H_{lz}^{life} - H_{lz}}{rt_{lz}^{life}}\right) \quad (21)$$

3.4. ESC 3

The third ESC, developed in detail in Ref. [20], attempts to reduce the utilization costs of the battery and hydrogen system. It, denoted as ESC,3 in the superscripts, presents a control scheme based on flowchart and fuzzy logic. The flowchart is responsible for deciding the power to be generated by/stored in the battery and/or hydrogen system while trying to minimize their utilization costs. The reference power defined by the flowchart control is supervised by a fuzzy logic controller in order to keep the battery SOC and hydrogen tank level between certain target margins.

4. Case study: off-grid HS located in Algeciras (Spain)

In order to check the performance of both ESC, an off-grid system located in Algeciras (Cádiz) Spain have been considered. The power demanded by this system during a day and throughout a year is shown in Fig. 4.

The consumption curve corresponds to a load in which the consumption peak occurs from 12.00 to 16.00 pm and it increases in spring and summer achieving a maximum demanded power around 1000 W.

The main characteristics of the battery, hydrogen system, WT and PV system are developed below. The sizing of these components has been performed by using Simulink Design Optimization (SDO) of MATLAB [30], mainly taking into account that the generated power must satisfy the demanded curve and extend the battery life.

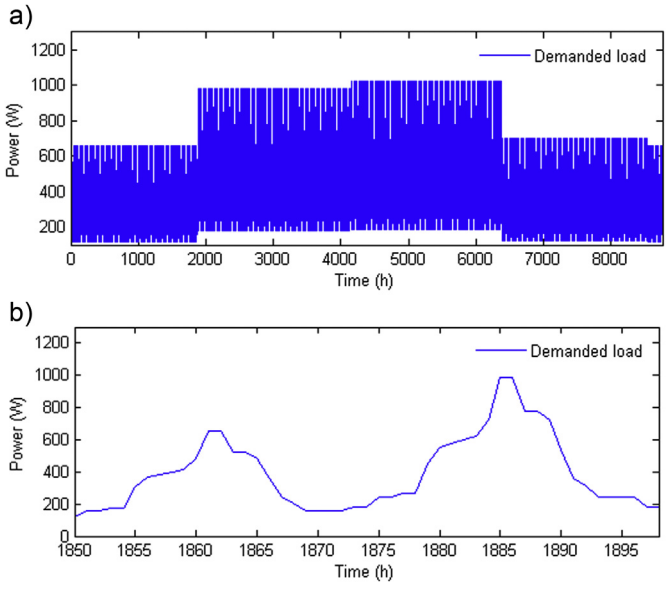

Fig. 4. Load power consumption during: a) two days; and b) one year.

4.1. Battery

The selected battery for the off-grid HS is a 660 Ah lead-acid battery. Its commercial name is BAE SECURA PVS, model PVS-660 [27], which is composed by 6 cells with a unit voltage of 2.23 V, so that the battery nominal energy (E_{bat}^{nom}) is 9500 Wh. Otherwise, as indicated in the battery datasheet, its maximum charge current is 330 A with a nominal charge power of about 4.3 kW, whose value is considered during the discharge process (P_{bat}^{max}). Regarding the battery life, the manufacturer ensures that the battery can complete 3150 cycles according to the IEC 61427 cycles, which has been considered as lifespan criteria (N_{cycles}^{life}).

With respect to the battery SOC, the manufacturer recommends avoid deep discharges of more than 80% (DOD_{nom}) representing a battery minimum SOC (SOC_{min}) of 20%. The battery SOC is calculated by Eq. (22). Hourly, it is obtained by means of an energy balance between the energy provided by and stored in the battery.

$$SOC(\%) = 100 \cdot \left(1 - \frac{1}{E_{bat}^{nom}} \sum P_{bat} \cdot t\right) \quad (22)$$

where P_{bat} is the power exchanged by the battery; and t is the duration of the power exchange (one hour).

4.2. Hydrogen system (fuel cell, electrolyzer and hydrogen tank)

The hydrogen system is composed of the following commercially available components: 1) The FC is a 1.2 kW polymer electrolyte membrane (PEM) FC from Heliocentris [31], model NEXA 1200; 2) the electrolyzer is the model HG-60 [29] from Heliocentris, which presents a nominal power consumption of 480 W with a nominal hydrogen generation of 60 standard liters h^{-1}; and 3) the metal hydride hydrogen tank has a total capacity of 760 L.

A mass balance between the hydrogen flow generated by the electrolyzer (q_{H2}^{gen}) and the hydrogen flow consumed by the FC (q_{H2}^{con}) is carried out every hour in order to obtain the hydrogen tank level. Compared with the battery SOC, the hydrogen tank can be discharged completely.

$$L_{H2}(\%) = 100\left[1 - \frac{1}{CAP_{H2}} \sum (q_{H2}^{gen} - q_{H2}^{con}) \cdot t\right] \quad (23)$$

With respect to the expected life of the elements, the manufacturer does not provide any information about the maximum working hours. The manufacturer gives information about the degradation rate. In the case of the FC, the output voltage is degraded 0.54 mV per each working hour, with an initial warranty of 1500 h. Thus, if a maximum degradation is fixed for the FC voltage, the FC lifetime can be calculated by Eq. (24). In this case, the allowed voltage drop has been fixed to a value which produces a very low output voltage but enough to make the FC DC/DC converter work properly.

$$H_{fc}^{life} = H_{warr} + \frac{V_{fc}^{loss}}{R_{fc}} \quad (24)$$

where H_{warr} is the FC working hours defined by the warranty [h]; V_{fc}^{loss} is the maximum voltage drop allowed in the FC output voltage [V]; and R_{fc} is the degradation rate of the FC voltage [V h^{-1}].

Similarly, the working hours deteriorate the performance of the electrolyzer. Thus, the electrolyzer will need to absorb more energy at the end of its life than at the beginning in order to produce the same hydrogen flow. Fixing a minimum efficiency in the electrolyzer, its lifespan in hours (H_{fc}^{life}) can be calculated as follows.

$$H_{lz}^{life} = \frac{R_{lz}^{\eta} - 1}{R_{lz}} \quad (25)$$

where R_{lz} is the degradation rate of the electrolyzer performance during an hour; and R_{lz}^{η} is the relationship between the electrolyzer nominal efficiency at beginning of its life and the minimum efficiency allowed.

4.3. Renewable energy system (WT and PV panels)

In the proposed HS, the renewable energy system is composed of WT and PV panels. These energy sources are independent of the ESC because they incorporate DC/DC converters with MPPT controller. Both energy sources generate the maximum energy available from the wind and sun irradiance. The ESC must have information every hour about the energy generated by them.

The selected WT is from Bornay [32] with a nominal power of 1.5 kW, and the PV system consists of nine EOPLLY [33] panels connected in parallel, with a total peak power of 1.62 kW p.

5. Simulation results and discussion

A comparative study between the two novel ESC presented in this work (ESC 1 and ESC 2) and the third ECS based on reducing the utilization costs (ESC 3) is carried out in this section. The controls are tested by simulation throughout the expected life (25 years) of the HS showed in Fig. 1 with the components described in Section 4. MATLAB-Simulink was used in the modeling and performed simulations, considering a sampling time of one hour.

The sun irradiance and the wind speed were taken throughout a year from a weather station located in Algeciras (Cádiz), Spain. These data (shown in Fig. 5) and the demanded load showed in Fig. 4 were extrapolated every year during 25 years.

Fig. 6 (Fig. 7) shows the power exchanged by the battery (hydrogen system) with the three ESC. Fig. 6a–c (Fig. 7a–c) represent the battery (hydrogen system) power throughout 25 years in the three ESC, and Fig. 6d (Fig. 7d) shows a detail of this power during two weeks. Fig. 8 shows the proportional constants of

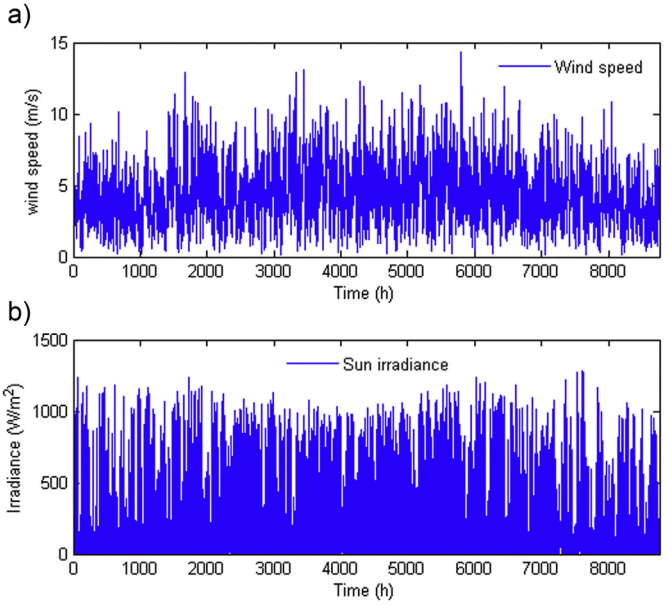

Fig. 5. a) Wind speed (m s^{-1}); and b) sun irradiance (kW m^{-2}).

the ESC 1 and ESC 2. In both controls, the battery and the hydrogen power are proportional to their constants and, in the case of ESC 1, they are directly related to the battery SOC and to the hydrogen level (Fig. 9).

In the ESC 1, the battery SOC and the hydrogen level vary in a similar way. Thus, during the discharges, the FC constant is around 0.68 and the battery constant around 0.32. On the other hand, during the charges, it occurs the following: 1) if the battery is charged and the hydrogen tank is not filled completely, because of the battery cannot absorb more energy, then $K_{bat,char} = 1$ and $K_{H2,char} = 0$; 2) if the hydrogen tank is completely charged and the battery can absorb more energy, then $K_{bat,char} = 0$ and $K_{H2,char} = 1$; and 3) if the battery and the hydrogen tank are charged, then $K_{bat,char} = K_{H2,char} = 0$, so that the available energy from the renewable energy sources cannot be stored.

Regarding the ESC 2, because the proportional constants depend on the lifetime of every component, its performance can be better observed throughout the simulation of 25 years. The lifetime evolution of the battery, FC and electrolyzer is represented for the ESC in Fig. 10. This ESC avoids the use of the components at the end of their life. Thus, Fig. 6b shows that, from around the year 8.5 to the year 10 and from the year 17 to the year 20, the battery is less used and the FC must generate more power than the rest of the time. The reason for this fact is that, during the time periods indicated, the remaining percentage of lifetime of battery, and thus the remaining available energy, is very small compared with the remaining percentage of lifetime of the FC and electrolyzer (Fig. 10). Furthermore, during those years, the battery suffers lower discharges and the hydrogen tank reaches very low levels (Fig. 9).

It can be observed that, with the ESC 3, the battery has to work delivering or absorbing small values of power (Fig. 6c), and

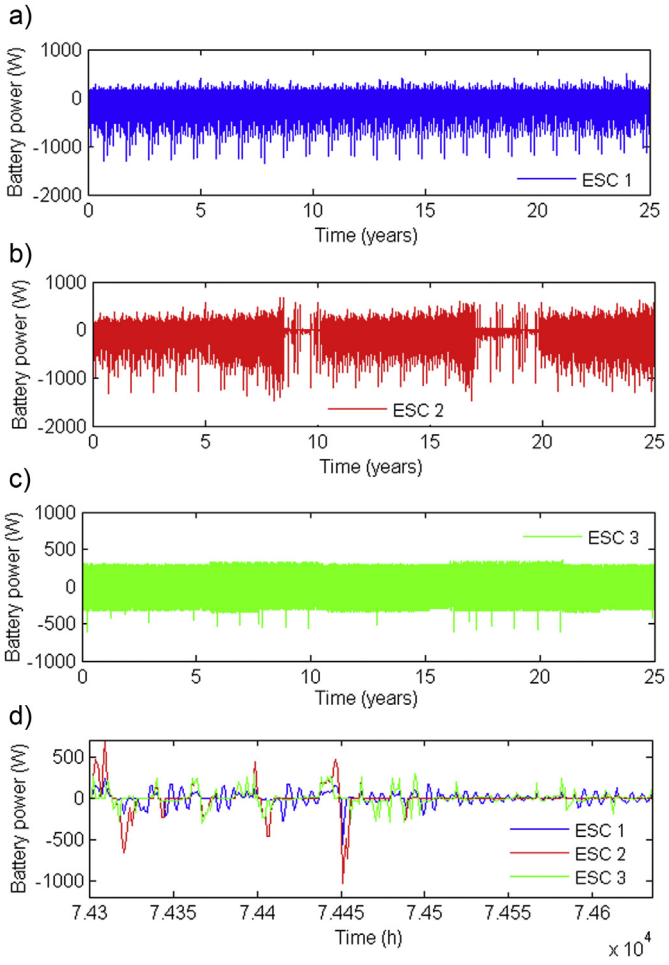

Fig. 6. Battery power: a) ESC 1 (25 years); b) ESC 2 (25 years); c) ESC 3 (25 years); and d) detail of two weeks.

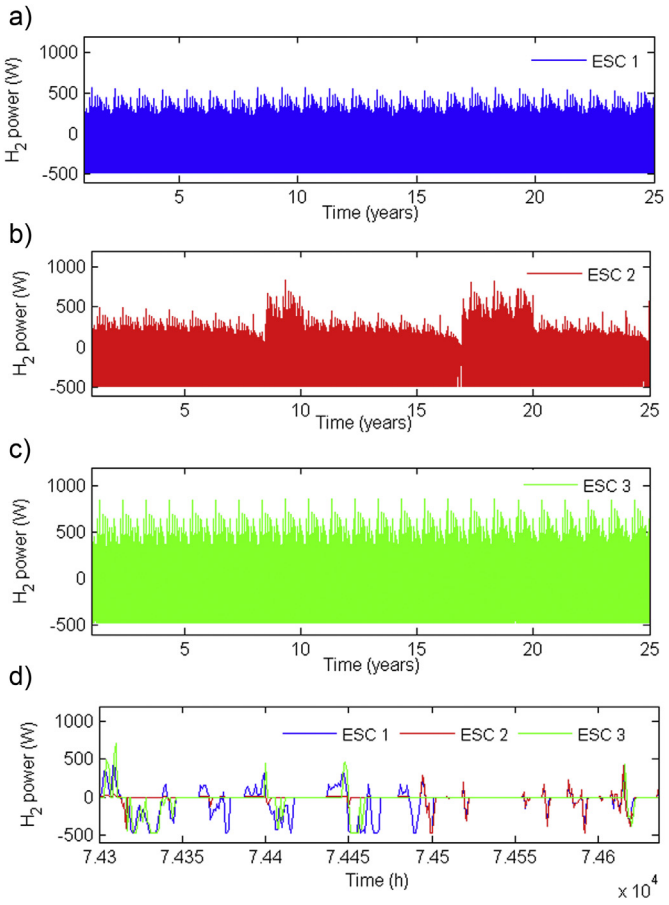

Fig. 7. Hydrogen system power: a) ESC 1 (25 years); b) ESC 2 (25 years); c) ESC 3 (25 years); and d) detail of two weeks.

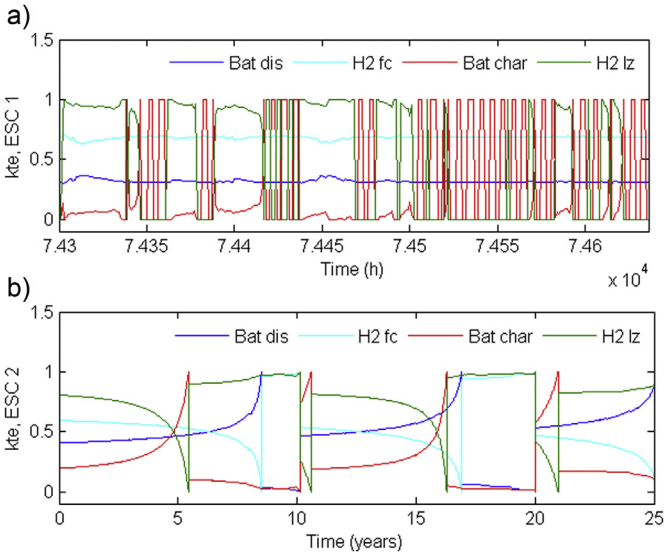

Fig. 8. Proportional constants: a) ESC 1 (two weeks); and b) ESC 2 (25 years).

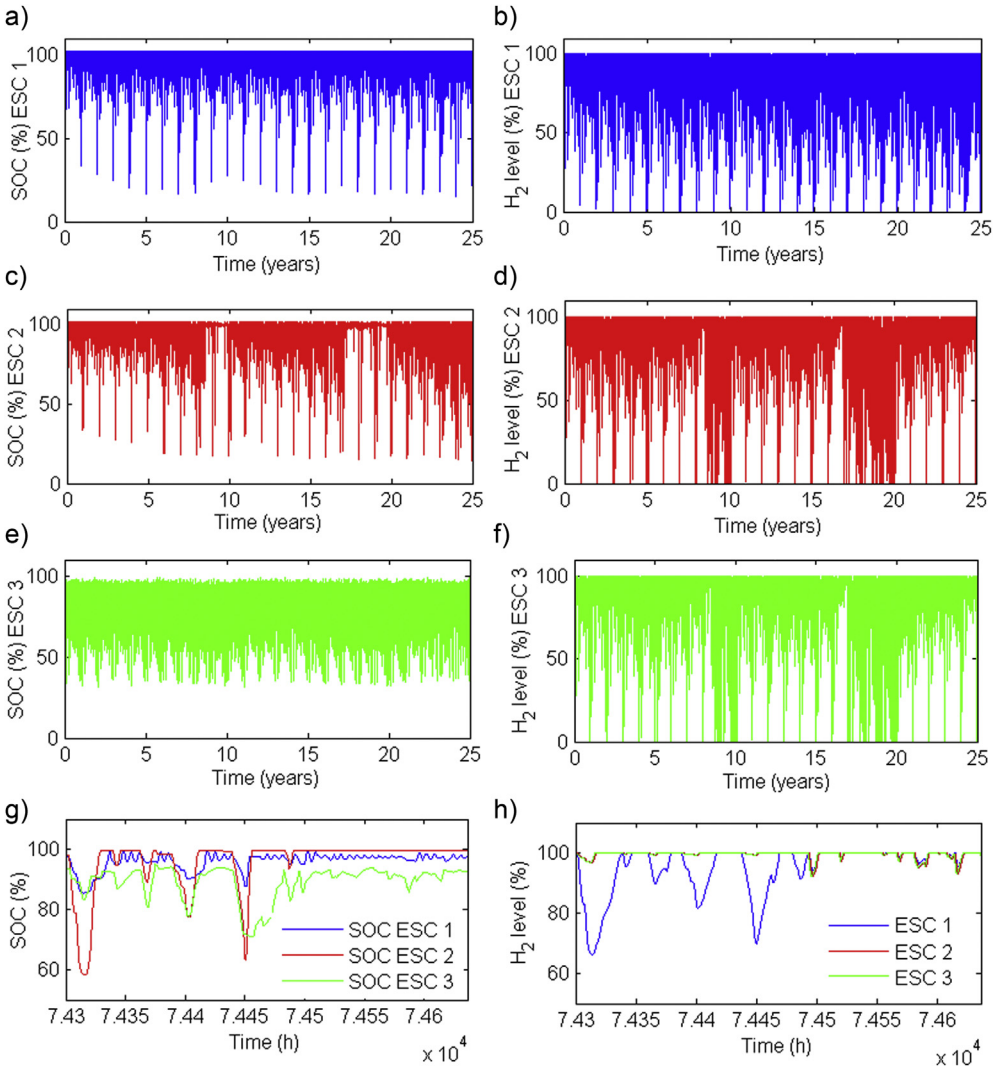

Fig. 9. a) Battery SOC with ESC 1 (25 years); b) hydrogen level with ESC 1 (25 years); c) battery SOC with ESC 2 (25 years); d) hydrogen level with ESC 2 (25 years); e) battery SOC with ESC 3 (25 years); f) hydrogen level with ESC 3 (25 years); g) detail of battery SOC (two weeks); and h) detail of hydrogen level (two weeks).

therefore, the power required from the hydrogen system is higher than in the other ESC (Fig. 7c). This is because when the power to be absorbed or generated is small, the battery utilization cost is lower than the hydrogen system utilization cost. On the contrary, if the power to be absorbed or generated is high, the cost of using the hydrogen system is cheaper than the battery. This causes that the hydrogen level presents deeper discharges than the battery SOC, as seen in Fig. 9e–f

Finally, the following parameters were calculated and studied in order to compare both ESC:

- Number of batteries, FC and electrolyzers used throughout the lifetime of the HS (N_{bat}, N_{fc}, and N_{lz}) and total number of components used (N_t).
- Unused energy (E_{un}), which is defined as the energy available from the renewable energy sources and not stored in the battery and/or in the hydrogen tank.
- Total time percentage that the ESC have been working in the states 4 and 8 (P_{48}), time percentage in the state 1 (P_1) and time percentage in the state 5 (P_5).
- Average and minimum values of the battery SOC and hydrogen level (SOC_{min}, SOC_{avg}, $H2_{min}$, and $H2_{avg}$).
- Battery efficiency (η_{bat}), hydrogen system efficiency (η_{H2}) and HS efficiency (η_{HS}), which were calculated by Eqs. (26)–(28).
- Total acquisition cost (Ac_t). This term is defined as the sum of the acquisition costs of the battery, FC and electrolyzer along 25 years and updated in every replacement by means of the annual interest rate.
- Average utilization cost (C^{av}_{used}). The utilization cost is calculated by Eq. (29), in which the utilization costs of battery (C_{bat}), FC (C_{fc}) and electrolyzer (C_{lz}) in every working hour are added. The utilization costs of the devices were calculated as defined in Ref. [20].

$$\eta_{bat} = \frac{\eta^2_{bat,con}\int_0^T P^{dis}_{bat}dt}{\int_0^T P^{char}_{bat}dt} \quad (26)$$

$$\eta_{H2} = \frac{\eta_{lz,con}\cdot\eta_{fc,con}\int_0^T P_{fc}dt}{\int_0^T P_{lz}dt} \quad (27)$$

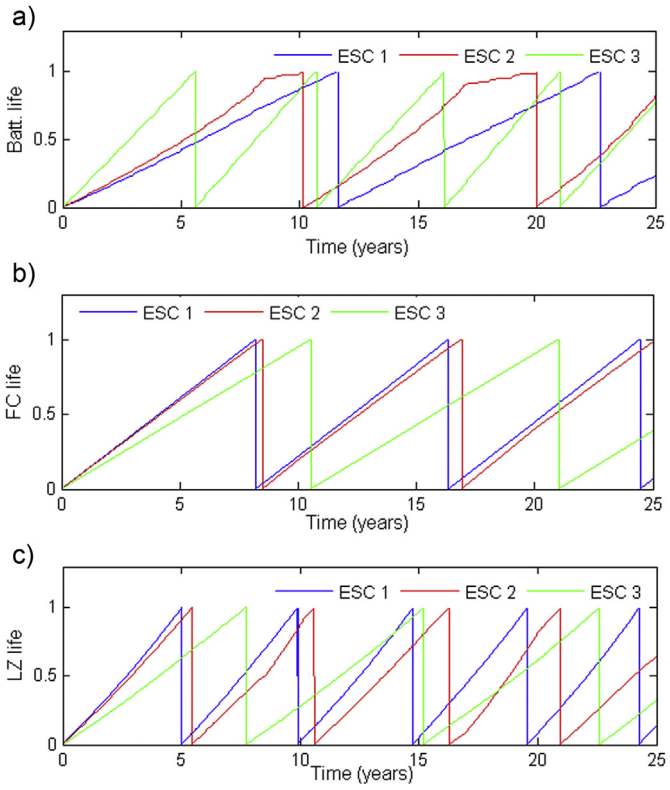

Fig. 10. Lifetime evolution (25 years): a) battery; b) FC; and c) electrolyzer.

$$\eta_{HS} = \frac{\int_0^T P_{load}\,dt}{\int_0^T (P_{wt}+P_{pv})dt + E_{low,H2}\int_0^T M_{H2}\,dt + \int_0^T P_{bat}\,dt} \quad (28)$$

$$C_{used} = C_{bat} + C_{fc} + C_{lz} \quad (29)$$

Table 2 shows the results of the comparison parameters obtained by each ESC. According to these results, it can be observed that, as expected, the ESC 2 needs less components during the lifetime of the HS. Nevertheless, with the ESC 2, the time percentage in the state 5, and thus the unused energy, are higher than with the ESC 1. Respect to the ESC 1, the working time in the states in which the control generates the ideal powers (states 4 and 8; $P_{48} = 64.4\%$) is higher than with the ESC 2. This is due to the fact that, in the ESC 1, the control of the battery SOC and hydrogen level is incorporated in the own control, and therefore the flowchart is less important. On the other hand, with respect to the efficiency parameters, the battery SOC and the hydrogen level present quite similar values. Hence, the HS efficiency reaches a value slightly greater than 50% (a little greater with the ESC 2), and the battery SOC is never below the 20%. Moreover, the minimum total acquisition cost is achieved with the ESC 2. This is mainly due to that less replacement are required with this ESC. However this fact does not imply that the average utilization cost achieved with this ESC is the lowest of all. Finally, as expected, the lowest average utilization cost is obtained with the ESC 3, however, this ESC presents the highest total acquisition cost and unused energy.

6. Conclusions

This paper has presented and compared two novel ESC applicable to off-grid HS based on renewable energy, hydrogen and battery. Furthermore, these ESC were also compared with a third ESC (ESC 3), whose control objective was to reduce the utilization costs of the energy storage devices.

Table 2
Results of the comparison parameters obtained by each ESC.

Parameter	Value		
	ESC 1	ESC 2	ESC 3
N_{bat}	3	3	5
N_{fc}	4	3	3
N_{lz}	6	5	4
N_t	13	11	12
E_{un} (kW h)	3650	4334	5443
P_{48} (%)	64.4	54.5	–
P_5 (%)	28.6	32.1	–
P_1 (%)	0	0	–
η_{bat} (%)	82.3	81.2	82.4
η_{H2} (%)	32.4	32.5	32.3
η_{HS} (%)	53.2	54.5	53.2
SOC_{min} (%)	21.2	20.5	20.6
SOC_{avg} (%)	94.9	95.8	82.94
$H2_{min}$ (%)	0	0	0
$H2_{avg}$ (%)	86.6	87.5	87.7
Ac_t	52,716	47,231	50,780
C^{av}_{used}	0.3467	0.3143	0.1523

The first ESC (ESC 1) improved the energy generated by the HS and stored in the energy storage devices, and thus, reducing the non-used energy. On the contrary, the second one (ESC 2), which considered the lifetime of the HS components, reduced the number of needed components along the expected life of the HS and improved the HS efficiency. Moreover, both ESC decided the battery power and the hydrogen system power (power generated by the FC or power absorbed by the electrolyzer) taking into account the net power (difference between the power generated by the renewable system and the demanded load), the battery SOC, the hydrogen tank level, and the remaining energy of the battery and hydrogen system. Depending on the ESC, these energies were the remaining energies in a charge or discharge cycle (ESC 1) or the total remaining energies which could be delivered or absorbed by the components during their lifetime (ESC 2). These energy parameters were not considered in the ESC 3, and however, the utilization costs of the energy storage devices were only used in the ESC 3.

The controls were tested along the expected lifetime of the HS with a demanded load that varied depending on the season of every year. The results demonstrated the feasibility of these ESC for off-grid applications. When the controls were compared, the ESC 2 showed better results, achieving higher HS efficiency than the other ESC, and reducing the number of needed components along the expected life of the HS. Nevertheless, the ESC 1 and ESC 2 did not improve the average utilization cost obtained with the ESC 3, since the utilization costs were not taken into account in these ESC.

Acknowledgment

This work was supported by the Spanish Ministry of Science and Innovation under Grant ENE2010-19744/ALT.

References

[1] R.M. Dell, D.A.J. Rand, J. Power Sources 100 (2001) 2–17.
[2] M. Reza, K. Mazlumi, A. Jalilvand, in: International Conference on Electrical and Electronics Engineering (ELECO), Bursa, Turkey, 2011, pp. 203–210.
[3] P. Thounthong, V. Chunkag, P. Sethakul, S. Sikkabut, S. Pierfederici, B. Davat, J. Power Sources 196 (2011) 313–324.
[4] T. Niknam, A. Kavousifard, S. Tabatabaei, J. Aghaei, J. Power Sources 196 (2011) 8881–8896.
[5] R. Sarrias, L.M. Fernandez, C.A. Garcia, F. Jurado, J. Power Sources 205 (2012) 354–366.

[6] M. Masih-Tehrani, M.-R. Ha'iri, V. Esfahanian, A. Safaei, J. Power Sources 244 (2013) 2–10.
[7] J. Zhu, M. Qiu, B. Wei, H. Zhang, X. Lai, W. Yuan, Energy 51 (2013) 184–192.
[8] C. Wang, M.H. Nehrir, IEEE Trans. Energy Convers. 23 (2008) 957–967.
[9] P.L. Zervas, H. Sarimveis, J.A. Palyvos, N.C.G. Markatos, J. Power Sources 181 (2008) 327–338.
[10] R. Dufo-López, J.M. Lujano-Rojas, J.L. Bernal-Agustín, Appl. Energy 115 (2014) 242–253.
[11] E. Dursun, O. Kilic, Electr. Power Energy Syst. 34 (2012) 81–89.
[12] S.B. Silva, M.M. Severino, M.A.G. de Oliveira, Renew. Energy 57 (2013) 384–389.
[13] A.U. Chavez-Ramirez, J.C. Cruz, R. Espinosa-Lumbreras, J. Ledesma-Garcia, S.M. Duron-Torres, L.G. Arriaga, Int. J. Hydrogen Energy 38 (2013) 12623–12633.
[14] T. Ma, H. Yang, L. Lu, Appl. Energy 112 (2013) 663–672.
[15] M. Castañeda, A. Cano, F. Jurado, H. Sanchez, L.M. Fernandez, Int. J. Hydrogen Energy 38 (2013) 3830–3845.
[16] K.-S. Jeong, W.-Y. Lee, C.-S. Kim, J. Power Sources 145 (2005) 319–326.
[17] B. Zhao, X. Zhang, P. Li, K. Wang, M. Xue, C. Wang, Appl. Energy 113 (2014) 1665–1666.
[18] D. Ipsakisa, S. Voutetakisa, P. Seferlisa, F. Stergiopoulosa, C. Elmasides, Int. J. Hydrogen Energy 34 (2009) 7081–7095.
[19] M.S. Carmeli, F. Castelli-Dezza, M. Mauri, G. Marchegiani, D. Rosati, Renew. Energy 41 (2012) 294–305.
[20] P. Garcia, J.P. Torreglosa, L.M. Fernandez, F. Jurado, Int. J. Hydrogen Energy 38 (2013) 14146–14158.
[21] O.C. Onar, M. Uzunoglu, M.S. Alam, J. Power Sources 161 (2006) 707–722.
[22] R. Dai, M. Mesbahi, Energy Convers. Manag. 73 (2013) 234–244.
[23] R.A. Gupta, R. Kumar, A.K. Bansal, in: International Conference on Computing, Communication and Applications (ICCCA), Dindigul, Tamilnadu, India, 2012, pp. 1–6.
[24] J.D. Maclay, J. Brouwer, G.S. Samuelsen, J. Power Sources 163 (2007) 916–925.
[25] R. Dufo-López, J.L. Bernal-Agustín, Renew. Energy 32 (2007) 1102–1126.
[26] R. Dufo-López, J.L. Bernal-Agustín, Sol. Energy 79 (2005) 33–46.
[27] Panasonic, Panasonic LC-XC1238, http://www.natbat.co.nz/uploads/F38-LC_XC1238.pdf.
[28] R. Dufo-López, J.L. Bernal-Agustín, Renew. Energy 33 (2008) 2559–2572.
[29] Heliocentris, Hydrogen Generator Datasheet, http://www.heliocentris.com/en/academia-offering/products/training-systems/hydrogen-supply/hydrogen-generator-hg.html.
[30] SimPowerSystems™, Reference, Hydro-Québec/The MathWorks, Inc., Natick, MA, 2010.
[31] Heliocentris, Nexa 1200 Datasheet, http://www.heliocentris.com/en/telecom-solutions/products/nexa-integration-kit/components.html.
[32] Bornay Aerogeneradores, WT 1500 Datasheet, http://www.bornay.com/eolica/en/wind-turbines/4/models/17/bornay-1500/2.
[33] ISOFOTON, ISF 215 PV Datasheet, http://www.isofoton.com/sites/default/files/ENG%20ISF%20215-220-225.pdf.